# Design, Synthesis, and Evaluation of Novel 3,6-Diaryl-4-aminoalkoxyquinolines as Selective Agonists of Somatostatin Receptor Subtype 2

Scott E. Wolkenberg,*,[†] Zhijian Zhao,[†] Catherine Thut,[‡,||] Jill W. Maxwell,[‡] Terrence P. McDonald,[‡] Fumi Kinose,[‡] Michael Reilly,[§,∞] Craig W. Lindsley,[†,⊥] and George D. Hartman[†]

Departments of [†]Medicinal Chemistry, [‡]Ophthalmics Research, and [§]Drug Metabolism, Merck Research Laboratories, Sumneytown Pike, P.O. Box 4, West Point, Pennsylvania 19486, United States

Ⓢ *Supporting Information*

ABSTRACT:
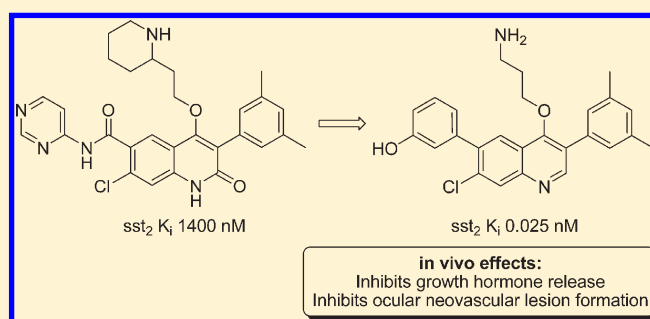
Agonists of somatostatin receptor subtype 2 (sst_2) have been proposed as therapeutics for the treatment of proliferative diabetic retinopathy and exudative age-related macular degeneration. An HTS screen identified 2-quinolones as weak agonists of sst_2, and these were optimized to provide small molecules with sst_2 binding and functional potency comparable to peptide agonists. Agonist **21** was shown to inhibit rat growth hormone secretion following systemic administration and to inhibit ocular neovascular lesion formation after local administration.

INTRODUCTION

Somatostatin is a peptide hormone secreted by the hypothalamus that signals through six receptor subtypes ($sst_{1,2A,2B,3-5}$) of the G protein-coupled receptor (GPCR) class.[1,2] Somatostatin has a wide variety of functions in the body, the most well-studied of which are its inhibitory actions on hormones of the pituitary/hypothalamic axis including thyroid stimulating hormone (TSH), growth hormone releasing hormone (GHRH), ghrelin, and growth hormone (GH). Recently, a variety of nonhormonal activities have been attributed to somatostatin as well, including roles in inflammation,[3,4] cell proliferation,[5] angiogenesis,[6,7] and neurotransmission.[1]

Somatostatin receptor subtype 2 (sst_2) mediates the inhibitory effects of somatostatin on GH, adrenocorticotropin, glucagon, vasoactive intestinal peptide, and gastric acid secretion. These actions have led a number of groups to seek to develop sst_2 selective agonists for the treatment of a variety of neuroendocrine tumors that result in acromegaly and diarrheas associated with carcinoid tumors and endocrine tumors producing vasoactive intestinal peptides (VIPomas). Early sst_2 agonists were peptide-based somatostatin analogues with improved plasma half-life ($t_{1/2}$ of several hours), potency, and selectivity (primarily sst_2 and sst_5)[8] versus endogenous somatostatin (plasma $t_{1/2} = 1-3$ min,

equal potency for $sst_{1,2A,2B,3-5}$).[9] Two such sst_2/sst_5 selective cyclic peptides, octreotide and lanreotide, are currently used for the management of acromegaly as well as carcinoid tumors and VIPomas. Despite their improved PK and selectivity versus somatostatin, both are delivered via intramuscular injection, and the development of novel orally bioavailable sst_2 agonists is desirable.

In addition to their established role in the treatment of acromegaly, sst_2 agonists have been proposed as therapeutics for the treatment of ocular angiogenic diseases such as proliferative diabetic retinopathy (PDR) and exudative age-related macular degeneration (wet AMD).[10] The role of somatostatin in these diseases is somewhat unclear, and its putative beneficial effects in these diseases could be mediated directly, via sst_2 expressed on retinal endothelial cells,[6] or indirectly via sst_2-dependent modulation of the GH–insulin-like growth factor 1 (IGF-1) axis.[11] Initial preclinical and clinical studies suggested that sst_2 agonists might inhibit and even regress PDR through its actions on GH release.[12,13] However, these initial findings have not been recapitulated in Ph 3 clinical trials. Recently, sst_2 expression on vascular

endothelial cells has been demonstrated, as has the ability of sst$_2$ agonists to inhibit endothelial cell proliferation, suggesting a potential non-GH dependent antiangiogenic mechanism.[6]

Herein, we describe the discovery and in vivo characterization of selective nonpeptide sst$_2$ agonists. Consistent with the reported effects of peptide sst$_2$ agonists, the novel agents suppress GH secretion in rats. In addition, they decrease neovascular lesions when administered locally to the eye in a rat choroidal neovascularization model.

■ RESULTS AND DISCUSSION

A high throughput screen of the Merck screening collection resulted in the identification of **1** as a modest affinity binder of sst$_2$ (Figure 1). The 3-aryl-4-aminoalkoxy-6-carboxamide series was originally discovered as gonadotropin-releasing hormone (GnRH) antagonists, and **1** exhibits potent GnRH activity.[14−18] Two modifications of this structure eliminate GnRH activity and dramatically increase affinity for sst$_2$: removal of the C6 carboxamide and removal of the C2 carbonyl. These beneficial changes were discovered serendipitously via sst$_2$ screening of compounds from this series prepared during the GnRH effort. Individually, these changes boost sst$_2$ binding potency by 1000- and 100-fold, respectively (see **2** and **3**) and when combined, as in **4**, an extremely potent sst$_2$ ligand results. This ligand also displays functional agonism, as **4** inhibits forskolin-stimulated cyclic adenosine monophosphate (cAMP) release with an IC$_{50}$ of 17 nM. In some cases, removal of the 7-chlorine is also tolerated (**5**) without deleterious effect on binding or functional potency (cAMP IC$_{50}$ = 7.6 nM) or selectivity (>250-fold vs sst$_{1,3−5}$).
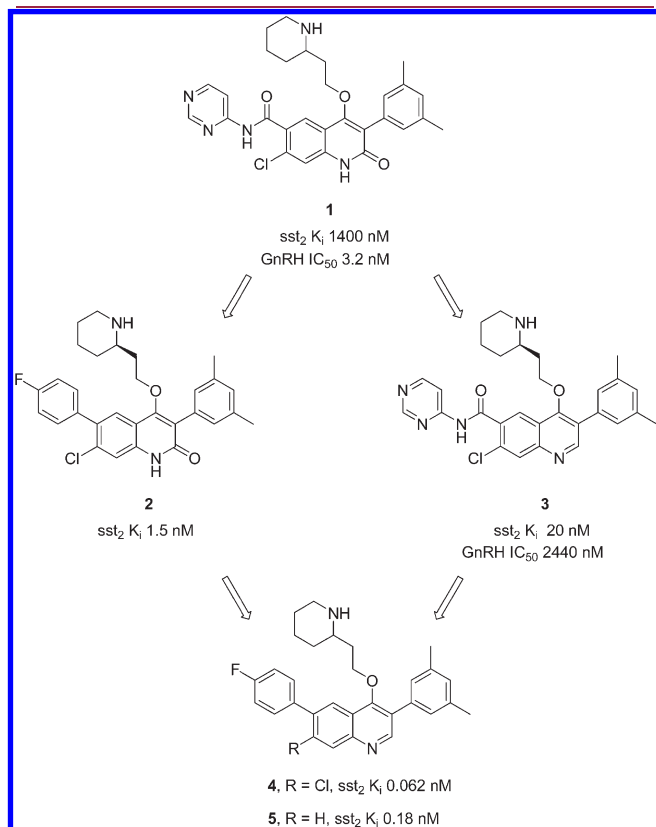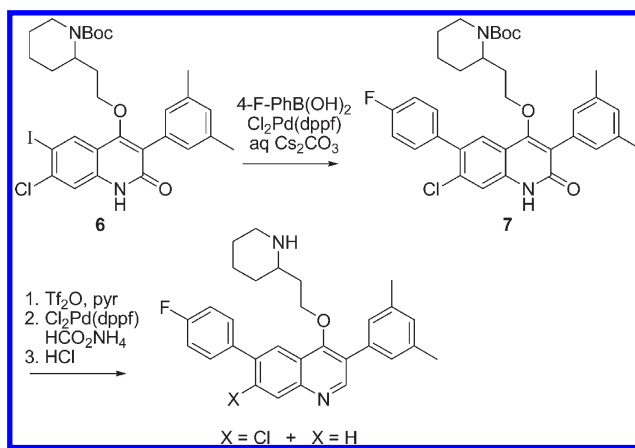

**Figure 1.** Screening lead and initial optimization.

Scheme 1. Initial Synthesis of Quinoline Compounds 4 and 5

Despite these advances upon simplification of **1−5**, further optimization was required, especially with regard to physical and pharmacokinetic properties. Compound **5** exhibits low aqueous solubility (<0.03 μg/mL at pH 7.4) and poor pharmacokinetics (e.g., dog Cl = 46 mL/min/kg), making it unsuitable for in vivo study, and an iterative analogue library approach was employed in its optimization.

Compounds **1−5** were prepared according to the route shown in Scheme 1, a slight modification of the published route used to synthesize GnRH inhibitors.[14,15,18] The advanced quinolone intermediate **6** was converted to biaryl **7** under Pd catalysis before being converted to its corresponding triflate. This intermediate could be converted to the 7-Cl and des-Cl analogues via partial or exhaustive reduction prior to Boc deprotection. This route efficiently provided the target compounds; however, the quinoline 3- and 6-aryl groups cannot be easily modified in parallel. To address this inefficiency, alternative syntheses of 4-alkoxy-3,6-biarylquinolines were utilized to prepare focused libraries of analogues.[19] These libraries typically contained 24−48 members and were prepared in an iterative fashion, with in vitro binding and functional data informing monomer selection in each round of synthesis.

Selected results for optimization of the 6-aryl group are presented in Table 1. Because of the objective of improving physical and pharmacokinetic properties, studies focused on heteroaromatics and carbocyclic aromatics bearing polar substituents. In terms of binding potency, both were well tolerated, providing sst$_2$ binders with affinity <1 nM. Five- and six-membered heteroaromatics and phenyl rings bearing hydrogen bond donating and accepting groups all provided very potent binders, and so long as an aromatic group was present, no significant steric or electronic effects were found. In contrast, functional potency varied, and in most cases, significant cAMP IC$_{50}$/K_i shifts (10−100-fold) were observed. The structure−activity relationship within the pyridine series at C6 (**8−14**) indicates that hydroxyl substitution (i.e., replacement of pyridine with pyridinone) is especially effective in reducing the shift between functional and binding potency (compare **8** and **9**). The effect is not reproduced with analogous amino substitution (compare **10** and **9**) or the corresponding phenol (**15**). The shifts observed could not be rationalized in terms of electronic effects or H-bond donors/acceptors, but a relationship between logD and functional/binding shifts was observed. Plotting the

Table 1. sst₂ Binding Affinities and Functional Potency for Test Compounds[a]
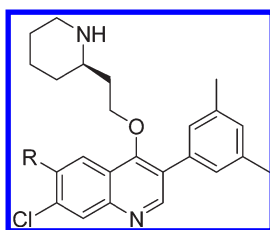
	R	sst$_2$ K_i (nM)	cAMP IC$_{50}$ (nM)
8		0.13	8.3
9		0.27	0.29
10		0.60	34
11		0.65	50
12		0.13	11
13		0.12	4.7
14		0.11	20
15		0.080	0.38
16		0.037	1.1
17		0.10	13
18		0.038	0.39
19		0.025	4.8
ent-(*S*)-**19**		1.5	145

[a] All compounds were >95% pure by HPLC and characterized by ¹H NMR and HRMS. Values represent the numerical average of at least two experiments. Interassay variability was ±25% for the binding assay (K_i) and for the cAMP assay (IC$_{50}$).

cAMP IC$_{50}$/K_i ratio as a function of logD (or, as in Figure 2, a larger set of calculated logD) reveals an apparent threshold ClogD below which minimal cAMP IC$_{50}$/K_i shifts are observed (threshold ClogD ~ 2.1 as indicated by the vertical line in Figure 2). The discovery of this threshold was facilitated by the parallel synthesis of >200 analogues and rapid assays for binding, functional potency, and logD. Apart from the relationship to
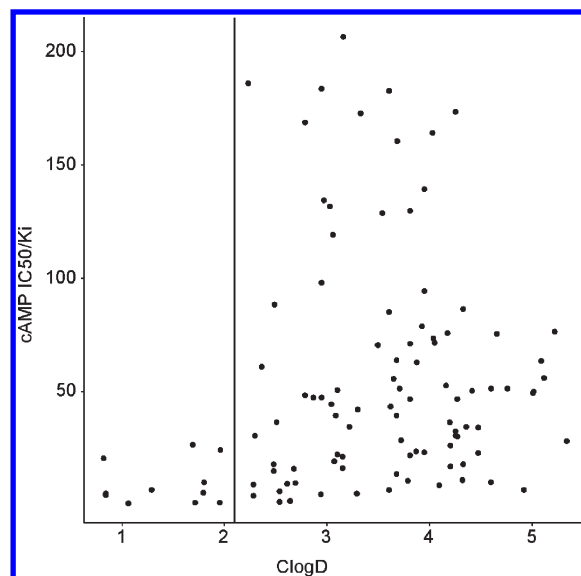
Figure 2. cAMP IC$_{50}$/K_i ratio as a function of ClogD.

logD, certain C6 aryl substituents increased binding potency so much that even with a 10-fold cAMP IC$_{50}$/K_i shift, very potent functional agonists were obtained (e.g., **15** and **18**). A general preference for the *R* stereochemistry at the piperidine C2 position was observed and is demonstrated by the 60-fold greater potency of **19** versus *ent*-(*S*)-**19**.
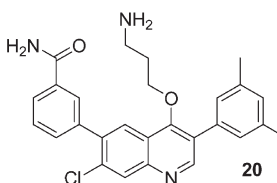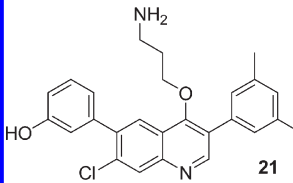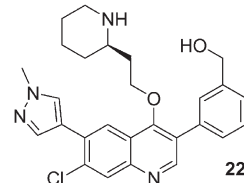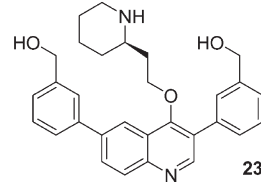
The quinoline 4-alkoxy substituent was varied via Mitsunobu etherification, and two acyclic aminopropyl ethers are shown in Table 2 (**20** and **21**). As was observed in the GnRH optimization of the related quinolone series,[14] these acyclic aminopropyl ethers retain potent binding and functional activity. Extension or truncation of the four atom chain linking the amine with the quinoline results in dramatic decreases in potency (data not shown), which suggests that these analogues bind within the well established somatostatin β-turn pharmacophore. Binding in this mode would require the aminoalkyl chain of **20** and **21** to occupy the same space as the side chain of somatostatin Lys⁹.[2] Substitution of the linking chain was not tolerated. Replacement of the 3,5-dimethylphenyl substituent at the quinoline C3 position was tolerated (see **22** and **23**), and 3-hydroxymethylphenyl provided near equivalent binding and functional potency.

Within the 3,6-diarylquinoline series, excellent selectivity versus other sst subtypes was observed (e.g., >1000-fold for **19** and **21**). Additionally, among selected agonists within this series, good selectivity versus off-target GPCRs was observed. In a screen of 116 GPCRs, **9** and **19** were found to bind to or inhibit 4 and 12 receptors with K_i or IC$_{50}$ values <1 uM, respectively.

The reductions in logD observed for compounds in Table 1 were accompanied by improvement in pharmacokinetic properties (see Table 3), and these compounds were suitable for dosing in rat pharmacodynamic studies. The moderate bioavailabilty observed with **19** and **21** is notable among small molecule sst ligands; while little published pharmacokinetic data are available, nonpeptide sst ligands have, to date, exhibited very low bioavailability.

To investigate the in vivo activity of compounds from this series, the ability of selected compounds to inhibit GH release was assessed in Sprague−Dawley rats. GH is secreted from the anterior pituitary gland in a pulsatile cycle that is controlled by GHRH and somatostatin,[20,21] and the resulting dynamic peaks

Table 2. sst$_2$ Binding Affinities and Functional Potency for Test Compounds^a

	sst$_2$ K$_i$ (nM)	cAMP IC$_{50}$ (nM)
20	0.080	0.38
21	0.025	4.8
22	0.13	8.3
23	0.13	11

^{a} All compounds were >95% pure by HPLC and characterized by ^{1}H NMR and HRMS. Values represent the numerical average of at least two experiments. Interassay variability was ±25% for the binding assay (K_i) and for the cAMP assay (IC$_{50}$).

Table 3. Pharmacokinetic Data for Selected Compounds

compound	species	Cl$_p$^{a}	t$_{1/2}$^{a}	Vd$_{ss}$^{a}	F^a (%)
9	dog^b	5.0	0.55	0.094	ND
19	rat^b	14	3.7	3.1	27
21	dog^c	7.1	11	5.7	ND
	rat^d	52	2.9	9.4	17

^{a} Plasma clearance (Cl$_p$) in mL/min/kg; plasma half-life ($t_{1/2}$) in h; steady-state volume of distribution (Vd$_{ss}$) in L/kg; and oral bioavailability (F). ^{b} 2 mg/kg iv dose and 10 mg/kg po dose. ^{c} 0.125 mg/kg iv dose. ^{d} 2 mg/kg iv dose and 5 mg/kg po dose.

and troughs of GH in the plasma can confound the in vivo assessment of the effects of sst$_2$ agonists on GH levels. To overcome this confounding factor, administration of a GH secretagogue was used to strongly increase the secretion of GH such that the normal GH pulses became insignificant. Importantly, GH secretion induced by GH secretagogues remains sensitive to the inhibitory effects of somatostatin.[22] To assess the in vivo effects of our sst$_2$ agonists, anesthetized rats were dosed intravenously with compound **21**, followed by a GH secretagogue challenge 50 min later. Plasma GH levels were measured every 5−15 min,[23] and the data were plotted as both plasma GH concentration as a function of time and as the area under the curve (AUC, Figure 3). In this model, **21** caused a

dose-dependent decrease in GH secretion (38 and 91% reduction in plasma GH AUC following administration of 0.2 and 2 mg/kg, respectively). Similar effects on GH secretion were seen with the sst$_2$ agonists **9** and **19** (data not shown). Administration of the peptide agonist octreotide (50 μg/kg resulted in a 99% reduction in plasma GH AUC). The in vivo potency of **21** approaches that of the octreotide, and taken together, the results demonstrate that **21** possesses potent in vivo GH suppressing activity.
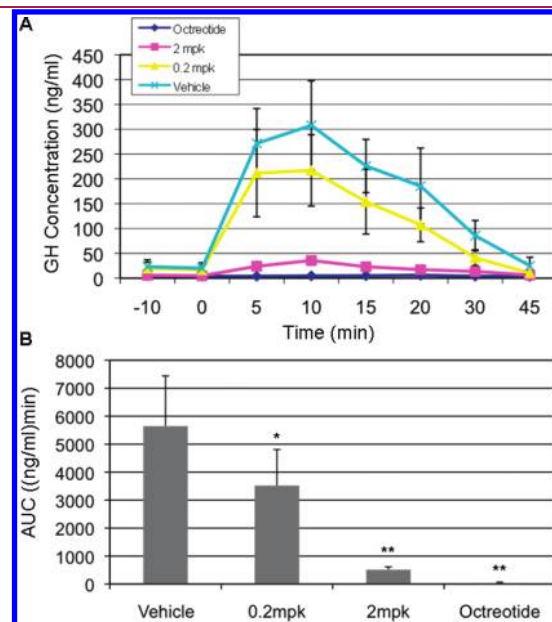

Figure 3. Effect of systemic administration of **21** on GH release. (A) Plasma GH concentration as a function of time following iv administration of octreotide (0.05 mg/kg) or **21** (0.2 and 2 mg/kg) at $t = -50$ min followed by GH secretagogue ($t = 0$ min). (B) AUC calculated from data in panel A for **21** (0.2 and 2 mg/kg) and octreotide (0.05 mg/kg). *$p < 0.05$. **$p < 0.005$.

The ability of sst$_2$ agonists to inhibit ocular neovascularization was studied in the rat laser-induced choroidal neovascularization model, a model that mimics aspects of wet AMD.[24] Local (intravitreal) dosing enabled an assessment of the effects of sst$_2$ agonists acting on receptors in the eye. Intraocular administration of **21** (5 or 15 μg) once every 4 days demonstrated a dose-dependent antiangiogenic effect as evidenced by a 35 and 53% reduction in neovascular lesion area with 5 or 15 μg per eye, respectively (Figure 4). The known antiangiogenic compound,
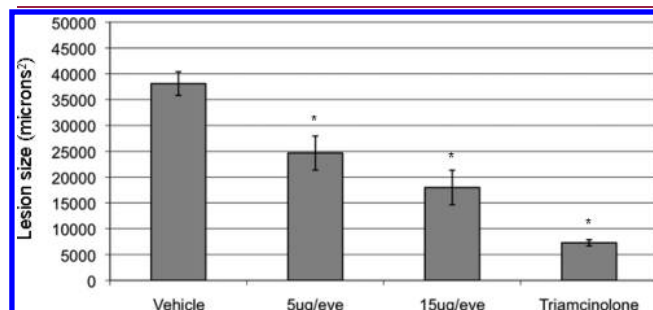

Figure 4. Effect of intraocular administration of **21** on ocular neovascular response. Neovasular lesion size following intraocular administration of **21** (5 or 15 μg/eye) or triamcinolone (50 μg/eye). See the text and ref 25. *$p < 0.005$.

triamcinolone acetonide, demonstrated an 81% reduction in neovascular lesion area at a dose of 50 μg/eye. The maximal antiangiogenic effects of **21** could not be determined as the maximum feasible dose of this compound was limited by its aqueous solubility. These results suggest that local delivery of sst$_2$ agonists could be useful for the treatment of neovascular eye diseases such as wet AMD and PDR.

The potential utility of sst$_2$ agonists for the treatment of ocular angiogenic diseases has been assessed clinically using the marketed peptides octreotide and lanreotide with mixed results. Several phase 2 studies of advanced nonproliferative diabetic retinopathy patients treated with octreotide showed encouraging reductions in disease progression;[12,13] however, the results of two subsequent prospective, controlled phase 3 studies were ambiguous.[25] Likewise, a small pilot study with lanreotide in patients with wet AMD suggested a potential positive impact on disease progression, but the trial was small, and the data did not reach statistical significance. It is worth noting that in the studies reported to date, octreotide and lanreotide were administered systemically, and controlled clinical trials in which sst$_2$ agonists are delivered locally to the eye have not yet been performed.

Our results suggest that local delivery of sst$_2$ agonists could be useful for the treatment of neovascular eye diseases, although further clinical studies will be necessary to fully elucidate the potential role for sst$_2$ agonists in the treatment of PDR and AMD. The 3,6-diarylquinoline agonists disclosed here represent useful tools for the preclinical study of sst$_2$, although further improvement in aqueous solubility may be needed to achieve maximal inhibition of ocular neovascularization and the development a potentially useful therapeutic.

■ EXPERIMENTAL SECTION

General Experimental Information. ^{1}H NMR spectra were recorded using Varian VXR spectrometers. Chemical shifts are reported in δ (ppm) using tetramethylsilane (δ 0 ppm) as an internal standard. High-resolution mass spectral data were obtained using a Bruker Daltonics FTICR/MS in electrospray ionization mode. HPLC spectra were obtained using Agilent 1100 HPLC systems. All animal studies were reviewed and approved by Merck's Institutional Animal Care and Use Committee.

Purity Determination. Analytical reversed phase high-performance liquid chromatography−mass spectrometry (LC-MS) was performed on an Agilent 1100 HPLC system equipped with an autosampler, a high-pressure pump (a binary pump was used), a single quadrupole mass spectrometer, and a photodiode array detector. The purity of the final compounds was determined using UV detection (λ = 214 nm). The chromatographic method employed the following: column, YMC J'sphere C18 (4 μM, 3.0 mm × 50 mm); mobile phase A, 0.05% TFA in water; mobile phase B, acetonitrile with 0.05% TFA; flow rate, 1.1 mL/min; elution profile, gradient elution from 5 to 100% B over 3.6 min followed by isocratic elution at 100% B for 0.45 min. According to these methods, purities for compounds **2**−**23** were >98%. Compounds **2**−**7** were prepared as described previously.[14−18]

7-Chloro-3-(3,5-dimethylphenyl)-6-(4-fluorophenyl)-4-{2-[(2R)-piperidin-2-yl]ethoxy}quinolin-2(1H)-one (2). ^{1}H NMR (CD$_3$OD, 500 MHz): δ 7.81 (s, 1H), 7.55 (s, 1H), 7.51−7.47 (m, 2H), 7.24−7.18 (m, 2H), 7.09 (s, 1H), 7.07 (s, 2H), 3.84 (dt, J = 10.2, 5.1 Hz, 1H), 3.77 (td, J = 9.3, 4.2 Hz, 1H), 2.94 (s, 1H), 2.87−2.76 (m, 1H), 2.39−2.32 (m, 7H), 2.02−1.94 (m, 1H), 1.83 (d, J = 14.5 Hz, 1H), 1.76 (d, J = 13.4 Hz, 1H), 1.72−1.63 (m, 1H), 1.62−1.49 (m, 2H), 1.39−1.29 (m, 1H), 1.22−1.12 (m, 1H). HRMS [M + H]$^+$ calculated, 505.2053; observed, 505.207.

7-Chloro-3-(3,5-dimethylphenyl)-4-{2-[(2R)-piperidin-2-yl]ethoxy}-N-(pyrimidin-4-yl)quinoline-6-carboxamide (3). ^{1}H NMR (CD$_3$OD, 500 MHz): δ 8.90 (s, 1H), 8.72 (d, J = 5.6 Hz, 1H), 8.35 (dd, J = 5.8, 1.4 Hz, 1H), 8.11 (s, 1H), 7.52 (s, 1H), 7.09 (d, J = 16.5 Hz, 5H), 3.89−3.74 (m, 2H), 3.03 (s, 1H), 2.94−2.82 (m, 1H), 2.38 (s, 6H), 2.09−1.94 (m, 2H), 1.89−1.50 (m, 5H), 1.47−1.34 (m, 1H), 1.26−1.14 (m, 1H). HRMS [M + H]$^+$ calculated, 532.211; observed, 532.2128.

7-Chloro-3-(3,5-dimethylphenyl)-6-(4-fluorophenyl)-4-{2-[(2R)-piperidin-2-yl]ethoxy}quinoline (4). ^{1}H NMR (CD$_3$OD, 500 MHz): δ 8.75 (s, 1H), 8.20 (s, 1H), 8.16 (s, 1H), 7.59−7.53 (m, 2H), 7.24 (t, J = 8.6 Hz, 4H), 7.13 (s, 1H), 3.89−3.85 (m, 2H), 2.90 (d, J = 12.1 Hz, 1H), 2.56−2.50 (m, 1H), 2.51−2.37 (m, 7H), 1.75−1.66 (m, 2H), 1.62−1.49 (m, 2H), 1.46 (d, J = 13.1 Hz, 1H), 1.38−1.17 (m, 2H), 1.00−0.90 (m, 1H). HRMS [M + H]$^+$ calculated, 489.2103; observed, 487.2101.

3-(3,5-Dimethylphenyl)-6-(4-fluorophenyl)-4-[2-(piperidin-2-yl)ethoxy]quinoline (5). ^{1}H NMR (CD$_3$OD, 500 MHz): δ 8.95−8.91 (m, 1H), 8.66 (d, J = 11.1 Hz, 1H), 8.44−8.28 (m, 2H), 8.19 (s, 2H), 7.94−7.89 (m, 2H), 7.41 (t, J = 8.7 Hz, 2H), 7.30 (s, 2H), 7.16 (s, 1H), 4.00−3.87 (m, 2H), 3.26 (d, J = 12.7 Hz, 1H) 3.13 (s, 1H), 2.87−2.76 (m, 1H), 2.39 (s, 6H), 2.12−2.04 (m, 1H), 1.81−1.60 (m, 4H), 1.56−1.44 (m, 1H), 1.38−1.15 (m, 2H). HRMS [M + H]$^+$ calculated, 455.2499; observed, 455.2493.

Analogues **8**−**23** were prepared according to the published synthetic route (see ref 19 and the Supporting Information, Scheme S1), and the general procedure is exemplified below for **19**.

7-Chloro-3-(3,5-dimethylphenyl)-4-{2-[(2R)-piperidin-2-yl]ethoxy}-6-(pyridin-3-yl)quinoline (8). ^{1}H NMR (CD$_3$OD, 500 MHz): δ 8.80 (s, 1H), 8.74 (dd, J = 2.3, 0.9 Hz, 1H), 8.65 (dd, J = 4.9, 1.6 Hz, 1H), 8.29 (s, 1H), 8.22 (s, 1H), 8.08 (dt, J = 7.9, 1.9 Hz, 1H), 7.61 (ddd, J = 7.9, 5.0, 0.9 Hz, 1H), 7.25 (s, 2H), 7.14 (s, 1H), 3.93−3.85 (m, 2H), 2.90 (d, J = 12.3 Hz, 1H), 2.57−2.50 (m, 1H), 2.51−2.39 (m, 7H), 1.75−1.66 (m, 2H), 1.63−1.44 (m, 3H), 1.38−1.28 (m, 1H), 1.27−1.17 (m, 1H), 0.99−0.90 (m, 1H). HRMS [M + H]$^+$ calculated, 472.2150; observed, 472.2160.

5-[7-Chloro-3-(3,5-dimethylphenyl)-4-{2-[(2R)-piperidin-2-yl]ethoxy}quinolin-6-yl]pyridin-2(1H)-one (9). ^{1}H NMR (CD$_3$OD, 500 MHz): δ 8.92 (s, 1H), 8.32 (s, 1H), 8.26 (s, 1H), 7.84 (dd, J = 9.4, 2.7 Hz, 1H), 7.72 (d, J = 2.6 Hz, 1H), 7.26 (s, 2H), 7.21 (s, 1H), 6.68 (d, J = 9.4 Hz, 1H), 4.10−3.99 (m, 2H), 3.34 (d, J = 13.0 Hz, 1H), 3.16 (s, 1H), 2.94−2.86 (m, 1H), 2.42 (s, 6H), 2.16−2.08 (m, 1H), 1.90−1.77 (m, 3H), 1.76 (d, J = 14.3 Hz, 1H), 1.66−1.55 (m, 1H), 1.50−1.38 (m, 1H), 1.38−1.26 (m, 1H). HRMS [M + H]$^+$ calculated, 488.2099; observed, 488.2107.

5-[7-Chloro-3-(3,5-dimethylphenyl)-4-{2-[(2R)-piperidin-2-yl]ethoxy}quinolin-6-yl]pyridin-2-amine (10). ^{1}H NMR (CD$_3$OD, 500 MHz): δ 8.79 (s, 1H), 8.56−8.55 (m, 1H), 8.29 (s, 1H), 8.21 (s, 1H), 8.05 (dd, J = 8.3, 2.5 Hz, 1H), 7.62 (dd, J = 8.3, 0.7 Hz, 1H), 7.25 (s, 2H), 7.14 (s, 1H), 3.93−3.85 (m, 2H), 2.91 (dd, J = 12.3, 3.0 Hz, 1H), 2.57−2.49 (m, 1H), 2.48−2.38 (m, 7H) 1.75−1.67 (m, 2H), 1.62−1.50 (m, 2H), 1.46 (d, J = 13.2 Hz, 1H), 1.38−1.28 (m, 1H), 1.28−1.17 (m, 1H), 1.01−0.91 (m, 1H). HRMS [M + H]$^+$ calculated, 487.2259; observed, 487.2261.

7-Chloro-3-(3,5-dimethylphenyl)-6-(6-methoxypyridin-3-yl)-4-{2-[(2R)-piperidin-2-yl]ethoxy}quinoline (11). ^{1}H NMR (CD$_3$OD, 500 MHz): δ 8.75 (s, 1H), 8.32−8.27 (m, 1H), 8.22 (s, 1H), 8.16 (s, 1H), 7.89 (dd, J = 8.6, 2.5 Hz, 1H), 7.24 (s, 2H), 7.13 (s, 1H), 6.93 (dd, J = 8.6, 0.8 Hz, 1H), 3.99 (s, 3H), 3.91−3.82 (m, 2H), 2.90 (dd, J = 12.2, 3.0 Hz, 1H), 2.57−2.52 (m, 1H), 2.51−2.37 (m, 7H), 1.76−1.66 (m, 2H), 1.63−1.49 (m, 2H), 1.46 (d, J = 13.2 Hz, 1H), 1.38−1.17 (m, 2H), 1.01−0.91 (m, 1H). HRMS [M + H]$^+$ calculated, 502.2256; observed, 502.2262.

7-Chloro-6-(6-chloropyridin-3-yl)-3-(3,5-dimethylphenyl)-4-{2-[(2R)-piperidin-2-yl]ethoxy}quinoline (12). ^{1}H NMR

(CD$_3$OD, 500 MHz): δ 8.79 (s, 1H), 8.56−8.55 (m, 1H), 8.29 (s, 1H), 8.21 (s, 1H), 8.05 (dd, J = 8.3, 2.5 Hz, 1H), 7.62 (dd, J = 8.3, 0.7 Hz, 1H), 7.25 (s, 2H), 7.14 (s, 1H), 3.93−3.85 (m, 2H), 2.91 (dd, J = 12.3, 3.0 Hz, 1H), 2.56−2.49 (m, 1H), 2.49−2.37 (m, 7H), 1.75−1.67 (m, 2H), 1.62−1.50 (m, 2H), 1.46 (d, J = 13.2 Hz, 1H), 1.38−1.25 (m, 1H), 1.26−1.17 (m, 1H), 1.01−0.91 (m, 1H). HRMS [M + H]$^+$ calculated, 506.1760; observed, 506.1768.

7-Chloro-3-(3,5-dimethylphenyl)-6-(6-fluoropyridin-3-yl)-4-[2-(piperidin-2-yl)ethoxy]quinoline (13). ^{1}H NMR (CD$_3$OD, 500 MHz): δ 8.79 (s, 1H), 8.38 (d, J = 2.5 Hz, 1H), 8.28 (s, 1H), 8.21−8.15 (m, 2H), 7.25−7.21 (m, 3H), 7.14 (s, 1H), 3.92−3.83 (m, 2H), 2.94−2.86 (m, 1H), 2.56−2.49 (m, 1H), 2.53−2.37 (m, 7H), 1.77−1.67 (m, 2H), 1.63−1.49 (m, 2H), 1.46 (d, J = 13.1 Hz, 1H), 1.38−1.25 (m, 1H), 1.26−1.18 (m, 1H), 1.00−0.90 (m, 1H). HRMS [M + H]$^+$ calculated, 490.2056; observed, 490.2064.

7-Chloro-3-(3,5-dimethylphenyl)-4-{2-[(2R)-piperidin-2-yl]ethoxy}-6-(pyridin-4-yl)quinoline (14). ^{1}H NMR (CD$_3$OD, 500 MHz): δ 8.80 (s, 1H), 8.69 (dd, J = 4.5, 1.7 Hz, 2H), 8.28 (s, 1H), 8.22 (s, 1H), 7.65 (dd, J = 7.6, 4.5 Hz, 2H), 7.25 (s, 2H), 7.14 (s, 1H), 3.92−3.84 (m, 2H), 2.90 (d, J = 12.2 Hz, 1H), 2.56−2.49 (m, 1H), 2.49−2.39 (m, 7H), 1.76−1.66 (m, 2H), 1.64−1.44 (m, 3H), 1.38−1.27 (m, 1H), 1.27−1.16 (m, 1H), 1.00−0.90 (m, 1H). HRMS [M + H]$^+$ calculated, 472.2150; observed, 472.2150.

4-[7-Chloro-3-(3,5-dimethylphenyl)-4-{2-[(2R)-piperidin-2-yl]ethoxy}quinolin-6-yl]phenol (15). ^{1}H NMR (CD$_3$OD, 500 MHz): δ 8.70 (s, 1H), 8.16 (s, 1H), 8.11 (s, 1H), 7.32−7.23 (m, 4H), 7.13 (s, 1H), 6.80 (d, J = 8.1 Hz, 2H), 3.90−3.83 (m, 2H), 2.91 (d, J = 12.2 Hz, 1H), 2.63−2.57 (m, 1H), 2.51−2.44 (m, 1H), 2.41 (s, 6H), 1.76−1.67 (m, 2H), 1.62−1.42 (m, 3H), 1.38−1.22 (m, 2H), 1.01−0.92 (m, 1H). HRMS [M + H]$^+$ calculated, 487.2147; observed, 487.2146.

3-[7-Chloro-3-(3,5-dimethylphenyl)-4-{2-[(2R)-piperidin-2-yl]ethoxy}quinolin-6-yl]phenol (16). ^{1}H NMR (CD$_3$OD, 500 MHz): δ 8.73 (s, 1H), 8.18 (s, 1H), 8.11 (s, 1H), 7.29−7.20 (m, 3H), 7.12 (s, 1H), 6.94−6.80 (m, 3H), 3.88−3.82 (m, 2H), 2.89 (d, J = 12.0 Hz, 1H), 2.55 (s, 1H), 2.60−2.28 (m, 7H), 1.75−1.64 (m, 2H), 1.61−1.43 (m, 3H), 1.38−1.17 (m, 2H), 1.00−0.90 (m, 1H). HRMS [M + H]$^+$ calculated, 487.2147; observed, 487.2149.

{4-[7-Chloro-3-(3,5-dimethylphenyl)-4-{2-[(2R)-piperidin-2-yl]ethoxy}quinolin-6-yl]phenyl}methanol (17). ^{1}H NMR (CD$_3$OD, 500 MHz): δ 8.75 (s, 1H), 8.21 (s, 1H), 8.16 (s, 1H), 7.55−7.47 (m, 4H), 7.25 (s, 2H), 7.14 (s, 1H), 4.71 (s, 2H), 3.92−3.84 (m, 2H), 2.89 (d, J = 12.1 Hz, 1H), 2.57−2.50 (m, 1H), 2.50−2.38 (m, 7H), 1.74−1.65 (m, 2H), 1.61−1.42 (m, 3H), 1.38−1.18 (m, 2H), 1.00−0.90 (m, 1H). HRMS [M + H]$^+$ calculated, 501.2303; observed, 501.2305.

3-{7-Chloro-3-(3,5-dimethylphenyl)-4-[2-(piperidin-2-yl)ethoxy]quinolin-6-yl}benzamide (18). ^{1}H NMR (CD$_3$OD, 500 MHz): δ 8.77 (s, 1H), 8.26 (s, 1H), 8.18 (s, 1H), 8.07 (d, J = 2.1 Hz, 1H), 8.01−7.97 (m, 1H), 7.74 (dd, J = 7.7, 1.7 Hz, 1H), 7.62 (t, J = 7.7 Hz, 1H), 7.25 (s, 2H), 7.14 (s, 1H), 3.92−3.83 (m, 2H), 2.88 (d, J = 12.1 Hz, 1H), 2.58−2.52 (m, 1H), 2.51−2.35 (m, 7H), 1.76−1.64 (m, 2H), 1.61−1.42 (m, 3H), 1.37−1.26 (m, 1H), 1.26−1.15 (m, 1H), 1.00−0.90 (m, 1H). HRMS [M + H]$^+$ calculated, 514.2256; observed, 514.2258.

General Procedure for the Syntheses of 8−23 (See the Supporting Information, Scheme S1, and Ref 19): Synthesis of 7-Chloro-3-(3,5-dimethylphenyl)-6-(1-methyl-1H-pyrazol-4-yl)-4-{2-[(2R)-piperidin-2-yl]ethoxy}quinoline (19). *Diethyl {[(3-Chloro-4-iodophenyl)amino]methylene}malonate (25; Supporting Information, Scheme S1).* Boiling chips were added to a mixture of 3-chloro-4-iodo-phenylamine (24, 260.0 g, 1.027 mol) and 2-ethoxymethylene-malonic acid diethyl ester (244.2 g, 1.130 mol), and the mixture was heated at 120 °C for 1 h with evolution of ethanol.

The warmed product 25 is used directly in next step (410 g, yield 95%). (The anilinoacrylate can be recrystallized from petroleum ether as slender white needles.) ^{1}H NMR (DMSO-d_6, 400 MHz): δ 10.55 (d, J = 14.0 Hz, 1H), 8.29 (d, J = 13.6 Hz, 1H), 7.83 (d, J = 8.8 Hz, 1H), 7.67 (d, J = 2.4 Hz, 1H), 7.10 (dd, J = 8.4, 2.4 Hz, 1H), 4.17 (q, J = 7.2 Hz, 2H), 4.09 (q, J = 7.2 Hz, 2H), 1.23 (d, J = 7.2 Hz, 3H), 1.19 (d, J = 7.2 Hz, 3H). ESI-MS m/z (M + H$^+$): 424.0, 426.0.

Ethyl 7-Chloro-4-hydroxy-6-iodoquinoline-3-carboxylate (26; Supporting Information, Scheme S1). Biphenyl ether (1.5 L) and compound 25 from the previous step were heated at reflux for 1 h before being cooled and filtered. The solids were washed with petroleum to obtain 26 (330.0 g, yield 90%). ESI-MS m/z (M + H$^+$): 377.9, 379.9.

7-Chloro-4-hydroxy-6-iodoquinoline-3-carboxylic Acid (27; Supporting Information, Scheme S1). Compound 26 (312.5 g, 0.827 mol) was mixed with 10% aqueous sodium hydroxide (1 L), and the mixture was heated at reflux until all solids dissolved. The reaction mixture was cooled, and the aqueous solution was separated from any oil present. The aqueous solution was acidified to pH 3, and solids were collected by filtration and washed with water until the filtrate measured pH 7. The solid was washed with two 2.5 L portions of methanol to remove the major impurities and provide pure 27 (281.7 g, yield 97%). ^{1}H NMR (DMSO-d_6, 400 MHz): δ 14.80 (br s, 1H), 12.40 (br s, 1H), 8.94 (s, 1H), 8.67 (s, 1H), 7.95 (s, 1H). ESI-MS m/z (M + H$^+$): 349.9, 351.9.

7-Chloro-6-iodoquinolin-4-ol (28; Supporting Information, Scheme S1). The carboxylic acid 27 (281.7 g, 0.806 mol) was suspended in biphenyl ether (1 L) and heated at reflux for 1 h before being cooled and filtered. The collected solids were washed with two 2.5 L portions of petroleum ether, two 2.5 L portions of methanol, two 2.5 L portions of water, and two 2.5 L portions of acetone to remove the major impurities and provide pure 28 (241.1 g, yield 97%). ^{1}H NMR (DMSO-d_6, 400 MHz): δ 11.85 (br s, 1H), 8.48 (s, 1H), 7.93 (d, J = 7.6 Hz, 1H), 7.72 (s, 1H), 6.06 (d, J = 7.2 Hz, 1H).

3-Bromo-7-chloro-6-iodoquinolin-4-ol (29; Supporting Information, Scheme S1). Compound 28 (120.0 g, 0.393 mol) was dissolved in acetic acid (1800 mL) and treated with NBS (70.0 g, 0.393 mol) before being heated at 60 °C for 2 h, cooled, and evaporated. Saturated aqueous NaHCO$_3$ was added, and the resulting solid was collected by filtration. The solid was washed with two 2.5 L portions of water and two 2.5 L portions of acetone to remove the major impurities and provide pure 29 (133.0 g, yield 88%). ^{1}H NMR (DMSO-d_6, 400 MHz): δ 8.52 (s, 1H), 8.49 (s, 1H), 7.74 (s, 1H). ESI-MS m/z (M + H$^+$): 383.8, 385.8, 387.8.

tert-Butyl(2R)-2-{2-[(3-bromo-7-chloro-6-iodoquinolin-4-yl)oxy]ethyl}piperidine-1-carboxylate (30; Supporting Information, Scheme S1). Quinolinol 29 (7.69 g, 30.0 mmol), tert-butyl(2R)-2-(2-hydroxyethyl)piperidine-1-carboxylate (4.59 g, 20.0 mmol), PPh$_3$ (6.30 g, 24.0 mmol), and THF (100 mL) were combined in a 500 mL round flask, which was sealed with a rubber stopper and sonicated for 3 min at room temperature. Sonication was stopped, and diisopropylazodicarboxylate (4.85 g, 24.0 mmol) was added via syringe over 10 min, after which the reaction was again sonicated for 40 min. During the sonication, all solids dissolved. After this period, THF was evaporated, and the residue was purified by flash chromatography (EtOAc/hexanes) to provide 30 as a yellow solid (7.39 g, 62%). ESI-MS m/z (M + H$^+$): 595.

tert-Butyl(2R)-2-(2-{[3-bromo-7-chloro-6-(1-methyl-1H-pyrazol-4-yl)quinolin-4-yl]oxy}ethyl)piperidine-1-carboxylate (31; Supporting Information, Scheme S1). A mixture of 30 (696 mg, 1 mmol), 1-methyl-4-(4,4,5,5-tetramethyl-1,3,2-dioxaborolan-2-yl)-1H-pyrazole (315 mg, 1.5 mmol), and Pd(dppf)Cl$_2$ dichloromethane adduct (40 mg, 0.05 mmol) in 1 M aqueous Cs$_2$CO$_3$ (5 mL) and THF (10 mL) was heated in a sealed 5 mL tube in a Biotage Initiator microwave at 80 °C for 15 min. The layers were separated, and the aqueous layer was extracted

with THF (2 × 5 mL). The combined THF solutions were concentrated, and the residue was dissolved in CH_2Cl_2 (150 mL), washed with brine, dried (Na_2SO_4), concentrated under reduced pressure, and purified by flash chromatography (SiO_2, EtOAc/hexanes) to afford **31** (452 mg, 83%). ESI-MS m/z (M + H$^+$): 493.

7-Chloro-3-(3,5-dimethylphenyl)-6-(1-methyl-1H-pyrazol-4-yl)-4-{2-[(2R)-piperidin-2-yl]ethoxy}quinoline (**19**). A mixture of **31** (55 mg, 0.1 mmol), 3,5-dimethylphenylboronic acid (20 mg, 0.13 mmol), and Pd(dppf)Cl$_2$ dichloromethane adduct (4 mg, 0.005 mmol) in 1 M aqueous Cs_2CO_3 (0.5 mL) and THF (2 mL) was heated in a sealed 5 mL tube in a Biotage Initiator microwave at 120 °C for 10 min. The layers were separated, and the aqueous layer was extracted with THF (2 × 2 mL). The combined THF solutions were treated with Quadra Pure TU for 2 h to remove Pd, before being filtered and concentrated under reduced pressure to afford a brown residue, which was treated with TFA/CH$_2$Cl$_2$ (1:1, 2 mL) and stirred at room temperature for 1 h. The reaction mixture was concentrated under reduced pressure and purified by LCMS to afford the pure **19** as a slightly yellow solid (TFA salt, 65 mg, 79%). ^{1}H NMR (CD$_3$OD, 600 MHz): δ 8.81 (s, 1H), 8.35 (s, 1H), 8.21 (s, 1H), 8.19 (s, 1H), 7.92 (s, 1H), 7.26 (s, 2H), 7.19 (s, 1H), 3.96–4.05 (m, 5H), 3.35 (d, J = 13.0 Hz, 1H), 3.14–3.20 (m, 1H), 2.92 (dt, J = 12.3, 2.9 Hz, 1H), 2.08–2.15 (m, 1H), 1.73–1.90 (m, 4H), 1.56–1.66 (m, 1H); 1.40–1.49 (m, 1H), 1.26–1.34 (m, 1H). HRMS m/z 475.2227 (C$_{28}$H$_{31}$ClN$_4$O + H$^+$ requires 475.2259).

3-[4-(3-Aminopropoxy)-7-chloro-3-(3,5-dimethylphenyl)quinolin-6-yl]benzamide (**20**). ^{1}H NMR (CD$_3$OD, 500 MHz): δ 8.83 (s, 1H), 8.07 (d, J = 8.6 Hz, 1H), 8.02 (t, J = 4.1 Hz, 1H), 7.96 (dt, J = 13.7, 3.0 Hz, 1H), 7.75 (d, J = 8.6 Hz, 1H), 7.68 (dt, J = 8.6, 1.1 Hz, 1H), 7.61 (t, J = 7.7 Hz, 1H), 7.28 (s, 2H), 7.16 (s, 1H), 3.82 (t, J = 5.8 Hz, 2H), 2.84 (t, J = 7.9 Hz, 2H), 1.98–1.90 (m, 2H). HRMS [M + H]$^+$ calculated, 460.1787; observed, 460.1809.

3-[4-(3-Aminopropoxy)-7-chloro-3-(3,5-dimethylphenyl)quinolin-6-yl]phenol (**21**). ^{1}H NMR (CD$_3$OD, 500 MHz): δ 8.77–8.73 (m, 1H), 8.24–8.16 (m, 1H), 8.14 (s, 1H), 7.33–7.27 (m, 1H), 7.25 (s, 2H), 7.13 (s, 1H), 6.98–6.92 (m, 2H), 6.89–6.86 (m, 1H), 3.87–3.82 (m, 2H), 2.74–2.68 (m, 2H), 2.41 (s, 6H), 1.83–1.75 (m, 2H). HRMS [M + H]$^+$ calculated, 433.1677; observed, 433.1671.

{3-[7-Chloro-6-(1-methyl-1H-pyrazol-4-yl)-4-{2-[(2R)-piperidin-2-yl]ethoxy}quinolin-3-yl]phenyl}methanol (**22**). ^{1}H NMR (CD$_3$OD, 500 MHz): δ 8.76 (s, 1H), 8.33 (s, 1H), 8.14 (d, J = 3.2 Hz, 2H), 7.91 (d, J = 0.8 Hz, 1H), 7.65 (s, 1H), 7.58–7.51 (m, 2H), 7.47 (d, J = 6.8 Hz, 1H), 4.72 (s, 2H), 4.00 (s, 3H), 3.93–3.83 (m, 2H), 2.98 (d, J = 12.3 Hz, 1H), 2.68–2.61 (m, 1H), 2.56 (td, J = 12.1, 2.9 Hz, 1H), 1.84–1.70 (m, 2H), 1.69–1.50 (m, 3H), 1.44–1.25 (m, 2H), 1.08–0.98 (m, 1H). HRMS [M + H]$^+$ calculated, 477.2057; observed, 477.2051.

[(4-{2-[(2R)-Piperidin-2-yl]ethoxy}quinoline-3,6-diyl)dibenzene-3,1-diyl]dimethanol (**23**). ^{1}H NMR (CD$_3$OD, 500 MHz): δ 8.78 (s, 1H), 8.46 (d, J = 1.7 Hz, 1H), 8.14–8.09 (m, 2H), 7.80 (s, 1H), 7.73–7.67 (m, 2H), 7.61–7.46 (m, 4H), 7.43 (d, J = 7.6 Hz, 1H), 4.74 (s, 4H), 3.99–3.88 (m, 2H), 3.12 (d, J = 12.5 Hz, 1H), 2.90 (s, 1H), 2.72 (td, J = 12.4, 3.0 Hz, 1H), 1.99–1.90 (m, 1H), 1.80–1.58 (m, 3H), 1.59–1.26 (m, 3H), 1.19–1.08 (m, 1H). HRMS [M + H]$^+$ calculated, 469.2486; observed, 469.2491.

Somatostatin Receptor Binding Assay. *Membrane Preparation.* Membranes for binding assays were prepared from CHO cells stably transfected with human sst$_1$, sst$_2$, sst$_3$, sst$_4$, or sst$_5$ expression constructs. Briefly, cells were washed in 1× CMF-PBS (10 mM HEPES, 1× Dulbecco's PBS) then in ice cold binding buffer (binding buffer: 50 mM Tris-HCl, pH 7.8, 5 mM MgCl$_2$, and 1 mM EGTA). The cells were collected in a small volume of binding buffer containing protease inhibitors (protease inhibitors: 10 μg/mL leupeptin, 10 μg/mL pepstatin, 200 μg/mL bacitracin, and 0.5 μg/mL aprotinin) and then centrifuged at 25000g for 10 min at 4 °C. The cell pellet was homogenized using a dounce homogenizer and centrifuged at 40000g for

30 min at 4 °C. Membranes were resuspended in fresh binding buffer containing protease inhibitors and stored at −70 °C.

Binding Assay Conditions. Final assay conditions for the receptor binding assay were 0–10000 nM compound, 0.1 nM ^{125}I-somatostatin-14 (Amersham, IM161), 2.5–50 μg membrane, and 0.5–2% DMSO to a final assay volume of 1 mL in binding buffer containing protease inhibitors. ^{125}I-somatostatin-14 and membranes were incubated for 30 min at room temperature followed by addition of compound resuspended in DMSO, and the mixture was incubated at room temperature for an additional 3 h with gentle shaking. Membrane-bound ^{125}I-somatostatin-14 was separated from unbound ^{125}I-somatostatin-14 by vacuum filtration through Packard Unifilter GF/B filter plates (Packard, 6005177) pretreated with 0.1% polyethyleneimine followed by washing with 5 mL of cold 50 mM Tris-HCl, pH 7.8. Sixty microliters of Microscint-20 scintillation fluid (Packard, 6013621) was added, and the bound ^{125}I-somatostatin-14 was quantitated using a Packard Topcount scintillation counter.

Inhibiton of Forskolin-Induced cAMP Release Assay. CHO cells expressing a Gα$_{qi5}$ subunit were grown to confluence in DMEM/F12 media (Cellgro, 16405CV) with 10% FBS (Gibco 16000044). Test compounds were added to the cell growth media to a final concentration of 0–10000 nM and incubated for 10 min at 37 °C. Forskolin (Sigma, F6886) was added to a final concentration of 12.5 μM, the cells were incubated at 37 °C for 40 min, and cAMP levels were assayed using a DiscoverX HitHunter cAMP kit (DiscoverX, catalog #900075) following the manufacturer's recommended protocol. Luminescence was measured using a GE Envision plate reader.

GH-Release Assay Protocol. Female Wistar rats (200–250 g) with indwelling jugular veinal and carotid arterial cannulas (ordered from Charles River Laboratories) were used. First, rats were anesthetized by IP injection with pentobarbital (Nembutal; 50 mg/kg). Once unconscious, vehicle, test compound, or octreotide (Amercian Peptide; 50 μg/kg) was delivered via jugular cannula. Control blood samples (0.3 mL) were collected via carotid cannula at 40 and 50 min post compound administration. A GH secretagogue was then delivered (10 μg/kg) via jugular cannula, and blood samples (0.3 mL) were collected via carotid cannula at 5, 10, 15, 20, 30, and 45 min post-GH secretagogue administration. Blood samples collected were centrifuged at 1600g for 20 min at 4 °C. Serum was removed and assayed for GH content by a double antibody RIA procedure.

Rat Laser Choroidal Neovascularization (CNV) Model Protocol. Male Brown Norway rats (175–225 g) from Charles River Laboratories were used. Animals were lasered and perfused as described previously.[24] Vehicle and test compound were administered via intravitreal injection. After lasering of anesthetized rat, a local anesthetic, 0.5% proparacaine HCl (Henry Schein), was administered to each eye. A 27G needle was used to make a small hole in the eye 3 mm posterior to iris angled 45° toward the optic nerve. A 30G blunt needle was then used to administer 5 μL vehicle (5% ethanol in PBS), test compound, or triamcinolone (Kenalog-10; Henry Schein) through the initial hole. Rats were injected days 0, 4, and 8 with vehicle or test compound, while triamcinolone was administered only on day 0.

■ ASSOCIATED CONTENT

S **Supporting Information.** Synthetic scheme for analogues **8**−**23**. This material is available free of charge via the Internet at http://pubs.acs.org.

■ AUTHOR INFORMATION

Corresponding Author
*Tel: 215-652-0821. Fax: 215-652-6345. E-mail: scott_wolkenberg@merck.com.

Present Addresses

‖Novartis Institutes of BioMedical Research, 220 Massachusetts Avenue, Cambridge, Massachusetts 02139.

∞GlaxoSmithKline, 1250 South Collegeville Road, Collegeville, PA 19426.

⊥Vanderbilt Program in Drug Discovery, Vanderbilt University Medical Center, Nashville, Tennessee 37232.

■ ABBREVIATIONS USED

sst_{1-5}, somatostatin receptor subtypes 1−5; GPCR, G protein-coupled receptor; TSH, thyroid stimulating hormone; GHRH, growth hormone releasing hormone; GH, growth hormone; VIPoma, endocrine tumor producing vasoactive intestinal peptide; PDR, proliferative diabetic retinopathy; AMD, age-related macular degeneration; IGF-1, insulin-like growth factor 1; GnRH, gonadotropin-releasing hormone; cAMP, cyclic adenosine monophosphate; AUC, area under the curve

■ REFERENCES

(1) Weckbecker, G.; Lewis, I.; Albert, R.; Schmid, H. A.; Hoyer, D.; Bruns, C. Opportunities in somatostatin research: Biological, chemical and therapeutic aspects. *Nat. Rev. Drug Discovery* **2003**, *2*, 999–1017.

(2) Wolkenberg, S. E.; Thut, C. J. Recent progress in the discovery of selective, non-peptide ligands of somatostatin receptors. *Curr. Opin. Drug Discovery Dev.* **2008**, *11*, 446–457.

(3) Karalis, K.; Mastorakos, G.; Chrousos, G. P.; Tolis, G. Somatostatin Analogs Suppress the Inflammatory Reaction in-Vivo. *J. Clin. Invest.* **1994**, *93*, 2000–2006.

(4) Weinstock, J. V.; Elliott, D. The somatostatin immunoregulatory circuit present at sites of chronic inflammation. *Eur. J. Endocrinol.* **2000**, *143*, S15–S19.

(5) Bousquet, C.; Puente, E.; Buscail, L.; Vaysse, N.; Susini, C. Antiproliferative effect of somatostatin and analogs. *Chemotherapy* **2001**, *47*, 30–39.

(6) Spraul, C. W.; Baldysiak-Figiel, A.; Lang, G. K.; Lang, G. E. Octreotide inhibits growth factor-induced bovine choriocapillary endothelial cells in vitro. *Graefes Arch. Clin. Exp. Ophthalmol.* **2002**, *240*, 227–231.

(7) Florio, T.; Morini, M.; Villa, V.; Arena, S.; Corsaro, A.; Thellung, S.; Culler, M. D.; Pfeffer, U.; Noonan, D. M.; Schettini, G.; Albini, A. Somatostatin inhibits tumor angiogenesis and growth via somatostatin receptor-3-mediated regulation of endothelial nitric oxide synthase and mitogen-activated protein kinase activities. *Endocrinology* **2003**, *144*, 1574–1584.

(8) Crider, A. M. Somatostatin receptor agonists and antagonists. *Expert Opin. Ther. Pat.* **2003**, *13*, 1427–1441.

(9) Patel, Y.; Wheatley, T. In vivo and in vitro plasma disappearance and metabolism of somatostatin-28 and somatostatin-14 in the rat. *Endocrinology* **1983**, *112*, 220–225.

(10) Papadaki, T.; Tsilimbaris, M.; Thermos, K.; Karavellas, M.; Samonakis, D.; Papadakis, A.; Linardakis, M.; Kouromalis, E.; Pallikaris, I. The Role of Lanreotide in the Treatment of Choroidal Neovascularization Secondary to Age-Related Macular Degeneration: A Pilot Clinical Trial. *Retina* **2003**, *23*, 800–807.

(11) Smith, L. E. H.; Kopchick, J. J.; Chen, W.; Knapp, J.; Kinose, F.; Daley, D.; Foley, E.; Smith, R. G.; Schaeffer, J. M. Essential Role of Growth Hormone in Ischemia-Induced Retinal Neovascularization. *Science* **1997**, *276*, 1706–1709.

(12) Grant, M. B.; Mames, R. N.; Fitzgerald, C.; Hazariwala, K. M.; Cooper-DeHoff, R.; Caballero, S.; Estes, K. S. The efficacy of octreotide in the therapy of severe nonproliferative and early proliferative diabetic retinopathy - A randomized controlled study. *Diabetes Care* **2000**, *23*, 504–509.

(13) Boehm, B. O.; Lang, G. K.; Jehle, P. M.; Feldmann, B.; Lang, G. E. Octreotide reduces vitreous hemorrhage and loss of visual acuity risk in patients with high-risk proliferative diabetic retinopathy. *Horm. Metab. Res.* **2001**, *33*, 300–306.

(14) DeVita, R. J.; Hollings, D. D.; Goulet, M. T.; Wyvratt, M. J.; Fisher, M. H.; Lo, J.-L.; Yang, Y. T.; Cheng, K.; Smith, R. G. Identification and initial structure-activity relationships of a novel non-peptide quinolone GnRH receptor antagonist. *Bioorg. Med. Chem. Lett.* **1999**, *9*, 2615–2620.

(15) DeVita, R. J.; Goulet, M. T.; Wyvratt, M. J.; Fisher, M. H.; Lo, J.-L.; Yang, Y. T.; Cheng, K.; Smith, R. G. Investigation of the 4-O-alkylamine substituent of non-peptide quinolone GnRH receptor antagonists. *Bioorg. Med. Chem. Lett.* **1999**, *9*, 2621–2624.

(16) Walsh, T. F.; Toupence, R. B.; Young, J. R.; Huang, S. X.; Ujjainwalla, F.; DeVita, R. J.; Goulet, M. T.; Wyvratt, M. J. J.; Fisher, M. H.; Lo, J.-L.; Ren, N.; Yudkovitz, J. B.; Yang, Y. T.; Cheng, K.; Smith, R. G. Potent antagonists of gonadotropin releasing hormone receptors derived from quinolone-6-carboxamides. *Bioorg. Med. Chem. Lett.* **2000**, *10*, 443–447.

(17) Young, J. R.; Huang, S. X.; Chen, I.; Walsh, T. F.; DeVita, R. J.; Wyvratt, M. J.; Goulet, M. T.; Ren, N.; Lo, J.-L.; Yang, Y. T.; Yudkovitz, J. B.; Cheng, K.; Smith, R. G. Quinolones as gonadotropin releasing hormone (GnRH) antagonists: Simultaneous optimization of the C(3)-aryl and C(6)-substituents. *Bioorg. Med. Chem. Lett.* **2000**, *10*, 1723–1727.

(18) DeVita, R. J.; Walsh, T. F.; Young, J. R.; Jiang, J.; Ujjainwalla, F.; Toupence, R. B.; Parikh, M.; Huang, S. X.; Fair, J. A.; Goulet, M. T.; Wyvratt, M. J.; Lo, J.-L.; Ren, N.; Yudkovitz, J. B.; Yang, Y. T.; Cheng, K.; Cui, J.; Mount, G.; Rohrer, S. P.; Schaeffer, J. M.; Rhodes, L.; Drisko, J. E.; McGowan, E.; MacIntyre, D. E.; Vincent, S.; Carlin, J. R.; Cameron, J.; Smith, R. G. A Potent, Nonpeptidyl 1*H*-Quinolone Antagonist for the Gonadotropin-Releasing Hormone Receptor. *J. Med. Chem.* **2001**, *44*, 917–922.

(19) Nolt, M. B.; Zhao, Z.; Wolkenberg, S. E. Controlled derivatization of polyhalogenated quinolines utilizing selective cross-coupling reactions. *Tetrahedron Lett.* **2008**, *49*, 3137–3141.

(20) Tannenbaum, G. S.; Martin, J. B. Evidence for an endogenous ultradian rhythm governing growth hormone secretion in the rat. *Endocrinology* **1976**, *98*, 562–570.

(21) Painson, J. C.; Tannenbaum, G. S. Sexual dimorphism of somatostatin and growth hormone-releasing factor in the control of pulsatile growth hormone secretion. *Endocrinology* **1991**, *128*, 2858–2866.

(22) Cheng, K.; Chan, W. W.; Butler, B.; Wei, L.; Schoen, W. R.; Wyvratt, M. J. J.; Fisher, M. H.; Smith, R. G. Stimulation of growth hormone release from rat primary pituitary cells by L-692,429, a novel non-peptidyl GH secretagogue. *Endocrinology* **1993**, *132*, 2729–2731.

(23) Clark, R. G.; Chambers, G.; Lewin, J.; Robinson, I. C. A. F. Automated repetitive microsampling of blood growth hormone profiles in conscious male rats. *J. Endocrinol.* **1986**, *111*, 27–35.

(24) Kinose, F.; Roscilli, G.; Lamartina, S.; Anderson, K. D.; Bonelli, F.; Spence, S. G.; Ciliberto, G.; Vogt, T. F.; Holder, D. J.; Toniatti, C.; Thut, C. J. Inhibition of retinal and choroidal neovascularization by a novel KDR kinase inhibitor. *Mol. Vis.* **2005**, *11*, 366–373.

(25) Palii, S. S.; Caballero, S., Jr.; Shapiro, G.; Grant, M. B. Medical treatment of diabetic retinopathy with somatostatin analogues. *Expert Opin. Invest. Drugs* **2007**, *16*, 73–82.